Turkish Journal of Engineering & Environmental Sciences

http://journals.tubitak.gov.tr/engineering/

Research Article

Turkish J Eng Env Sci
(2014) 38: 455 – 479

doi:10.3906/muh-1402-3

Kinetics and equilibrium modeling of lead(II) and chromium(III) ions' adsorption onto clay from Kono-bowe, Nigeria

Regina Obiageli AJEMBA*
Department of Chemical Engineering, Nnamdi Azikiwe University, Awka, Nigeria

Received: 08.02.2014 • **Accepted/Published Online:** 30.01.2016 • **Printed:** 04.03.2016

Abstract: Clay from Kono-bowe, Nigeria, was activated thermally and chemically and used to remove lead(II) and chromium(III) ions from aqueous solution. The effects of adsorption process variables were studied as well as the kinetics and equilibrium of the process. Analysis of the activated samples showed that the surface area, cation exchange capacity, and adsorption performance were positively favored by both activation processes. It was observed that the adsorption rate increased with an increase in temperature, contact time, adsorbent dosage, initial ion concentration, and solution pH values. The pH_{PZC} of the adsorbents was determined to be 6.5, 7.4, and 7.2, for KBR, KBTA, and KBAA, respectively. It was observed that sample KBAA yielded maximum adsorption efficiency of 99.9% for the removal of chromium(III), and gave maximum adsorption efficiency of 98.7% for lead(II) removal. The results of the kinetics analysis of the adsorption data revealed that adsorption follows pseudo-second-order kinetics. Analysis of the equilibrium data showed that the Langmuir isotherm provided a better fit to the experimental data for KBR, while the Freundlich isotherm fitted the experimental data of KBTA and KBAA. Evaluation of the thermodynamic parameters revealed that the adsorption process is spontaneous and endothermic.

Key words: Adsorption, clay activation, modeling, kinetics, equilibrium, isotherm

1. Introduction

The presence of heavy metals in drinking water sources and in edible agricultural crops can be harmful to human beings. It is well known that heavy metals can be toxic, e.g. they damage the nerves, liver, and bones and they block functional groups of vital enzymes [1]. Heavy metals are found in water, air, and soil. The major sources of heavy metals in water and soil are wastewater streams from many industrial processes [2]. Heavy metals like chromium, copper, lead, zinc, mercury, and cadmium are present in wastewater from several industries such as metal cleaning and plating baths, refineries, paper and pulp, tanning, dyes and pigments, wood preserving, glass, ceramic paints, and chemical manufacturing.

There are many conventional processes for the removal of toxic ions from water, which include chemical precipitation, coagulation, reverse osmosis, ion-flotation, evaporation, ion-exchange, and adsorption [3,4]. Most of these methods suffer from drawbacks such as incomplete metal removal, high capital and operational costs, requirements of expensive equipment and monitoring system, high reagent and energy requirements, generation of toxic sludge, other waste products that require disposal, membrane scaling, fouling, and blocking [5,6]. Adsorption methods were found to be more effective and attractive due to their lower costs and high efficiency of heavy metal ion removal. Activated carbon is a potential adsorbent for the removal of several organic and

*Correspondence: ginaajemba@rocketmail.com

inorganic pollutants. The adsorption process has been widely used all over the world and various adsorbents have been used for removal of heavy metal ions like silica gel, polymer, carbon nanotubes, fly ash, clays, zeolites, chitosan, peat moss, biosorbent, and food waste. In recent years, researchers have developed many adsorbents; sometimes the adsorbent is used as it is or impregnated or modified to improve the capacity of the adsorption. Several types of adsorbents are developed to get enhanced adsorption capacity in an inexpensive way. In this invention many researchers have contributed to the development of adsorbents from natural sources, industrial wastes, agricultural wastes, food waste, etc. Amongst the various adsorbents, the application of different types of local clays is the oldest.

Clays are well-known adsorbents used for heavy metal removal. Acid and other reagents are used for activation of clays. The clays are extremely fine particles exhibiting chemical properties of colloids. Kaolinite and its modified forms, acid-activated kaolinite, poly (oxo-zirconium) kaolinite, and tetra-butyl-ammonium kaolinite, were investigated by Bhattacharyya and Sharma [7] for adsorption of Cr(VI). The Langmuir monolayer capacity of the clay adsorbents is from 10.6 to 13.9 mg/g [8]. Acid activation of Resadiye clays and Hancili clays was done with H_2SO_4 and HCl; adsorption capacity was found to be 1.40, 0.75, and 0.884 mg/g for H, H-HCl, and H-H_2SO_4 and 1.85, 1.44, and 2.20 mg/g for R, R-HCl, and R-H_2SO_4, respectively [9]. Bentonite clay has been modified by several treatments such as aluminum pillaring, acid activation, and pillaring followed by acid activation, which shows 50 to 113 mg/g adsorption capacity [10]. Sharma and Wang [11] used indigenous clay, i.e. china clay, as adsorbent and 80.3% removal at low concentration of metal ion was reported at pH 6.5 [12,13]. Local illitic clay, from Jebel Tejra located in southwest Tunisia in North Africa was studied for removal of Cr(III) and Cd(II) and found to show 35.70 mg/g and 52.5 mg/g adsorption capacity, respectively. In that study 20 h was required for maximum adsorption [14]. Brazilian vermiculite was used for the removal of specific toxic metals as zinc, cadmium, chromium, and manganese from aqueous solution. Amongst all, Cd(II) was maximally adsorbed to 63.281 mg/g, while Cr(III), Zn(II), and Mn(II) were reported as 39.05, 41.77, and 31.53 mg/g [15]. All over the world many studies have been conducted on heavy metal sorption using clay mineral [16–22]. The most important parameters controlling heavy metal adsorption and their distribution between clay and water are clay type, metal speciation, metal concentration, pH, solid/liquid ratio, and contact time [23–26]. Of all these factors, pH is considered the master variable controlling ion exchange, dissolution/precipitation, reduction/oxidation, adsorption, and complex formation reactions.

In the present study, clay from Kono-bowe, Nigeria, was activated thermally and chemically with sulfuric acid and used to remove lead(II) and chromium(III) ions from aqueous solution. Physicochemical properties of the raw and activated clay sorbents were analyzed. The adsorption isotherm, kinetics, and thermodynamic models were discussed successively. The sorbent produced from the chemically activated sample was found to be economical and of good quality for the removal of heavy metal ions from contaminated water.

2. Experimental procedures

2.1. Preparation of the sorbent

The clay used in this study was mined from Kono-Bowe (N: 8°32'05"; E: 8°55'05"; A: 126 m) in River State, Nigeria. The mined clay was sun-dried for 48 h and ground to smaller particles using a mortar and pestle. The raw ground clay was then subjected to different modification processes, while some part was reserved for the analysis and labeled as KBR.

2.2. Modification methods

2.2.1. Thermal activation

The physical modification of the raw clay was performed by thermal activation. The preparation of the raw clay was done by calcination in a muffle furnace. The calcination was carried out at 400 °C. The process of thermal activation was done by measuring out 10 g of raw bentonite in a crucible and heating in the muffle furnace. The temperature of the muffle furnace was allowed to rise steadily to the desired value and the heating was done for 2 h. At the completion of the time, the samples were withdrawn from the furnace and cooled in a desiccator for 2 h 30 min. The thermal activated sample was labeled KBTA.

2.2.2. Acid activation

The raw clay was treated with 0.75 mol/L sulfuric acid solution at 60 °C. Then 10 g of the raw clay was reacted with 100 mL of known concentration of sulfuric acid solution in a rotary shaker with temperature and agitation control for 3 h. At the completion of the reaction period, the reaction was terminated and the slurry was filtered. The acidified product was then washed several times with distilled water until the filtrate was free of sulfate ions. The residue was then dried in an oven at 80 °C for 24 h. The acid activated sample was labeled KBAA.

2.3. Preparation of aqueous solutions

Aqueous solutions of lead(II) and chromium(III) were prepared from their nitrate salts of analytical grade reagent, Pb $(NO_3)_2$ and Cr $(NO_3)_3.9H_2O$ (all with declared impurity of less than 0.5%).

2.4. Batch adsorption studies

The adsorption of lead(II) and chromium(III) onto raw and activated Kono-bowe (KBR, KBAA, and KBTA) clay was studied in the following manner. Batch adsorption isotherm experiments were conducted by varying concentrations of Pb(II) and Cr(III) from 100 mg/L to 500 mg/L, at constant adsorbent dose of 5 g and agitation speed of 320 rpm. Adsorbent dosage was varied from 0.5 g to 5 g at constant concentration of Pb(II) and Cr(III) of 100 mg/L. The effects of contact time and pH were studied with Pb(II) and Cr(III) concentration of 100 mg/L and adsorbent dosage of 5 g. Contact time was varied from 15 min to 270 min, while pH value was varied from 2 to 10, respectively. A measured quantity of the adsorbent was added to 50 mL of solution of the prepared metal solution in 250-mL Erlenmeyer flasks. The mixture was agitated in an incubated shaker at a predetermined temperature and speed for the desired time. At the completion of the reaction period, the supernatant was separated by centrifugation at 3000 rpm for 15 min and the residual concentration in the supernatant was determined. The metal concentration in the raw and treated samples was determined by atomic absorption spectrophotometer (model WFJ 525). The response, removal efficiency of the metal ions by the adsorbent, was calculated as

$$Y\,(\%) = 100\frac{c_0 - c_i}{c_0}, \tag{1}$$

where c_0 and c_i are the initial and final concentration of the metal ion solution.

The amount of equilibrium adsorption, q_e (mg/g), was calculated by

$$q_e = \frac{V\,(c_0 - c_e)}{M}, \tag{2}$$

where c_0 and c_e (mg/L) are the liquid-phase concentrations of metal ions initiallly and at equilibrium, respectively, V (L) is the volume of the solution, and M (g) is the mass of dry prepared sorbent used.

2.5. Determination of pH point of zero charge (pH_{PZC})

The pH point of zero surface charge characteristics of the adsorbents (KBR, KBAA, and KBTA) was determined using the solid addition method [27,28]. First 40 mL of 0.1 M NaCl solution was transferred to a series of 250-mL stoppered conical flasks. The pH_i values of the solutions were then adjusted to between 2 and 10 by adding NaOH and were measured using a Consort C931 pH meter (Belgium). The total volume of the solution in each flask was adjusted to exactly 50 cm^3 by adding NaCl solution of the same strength. The pH_i of the solution was then accurately noted. Next 0.5 g of the adsorbents was added in turn to each flask, and the flask was securely capped immediately. The suspensions were then kept shaking for 24 h and allowed to equilibrate for 0.5 h. The final pH values of the supernatant liquids were noted. The difference between the initial and final pH (pH_f) values (ΔpH) was plotted against the pH_i. The point of intersection of the resulting curve with the pH_i axis, i.e. at $\Delta pH = 0$, gave the pH_{PZC}.

2.6. Isothermal and kinetic studies

The effect of contact time on the adsorption of lead(II) and chromium(III) ions was analyzed by evaluating the kinetic data by pseudo-first-order, pseudo-second-order, Elovich, Bangham, and intraparticle kinetic models. The adsorption isotherms were evaluated to analyze the equilibrium data. The adsorption isotherm is the equilibrium relationship between the concentration in the liquid phase and the concentration in the solid phase in the adsorbate particles at a given temperature [29]. The experimental data obtained were analyzed by Langmuir, Freundlich, Dubinin–Radushkevich, Harkin–Jura, and Temkin adsorption isotherm models.

3. Results and discussion

3.1. Characterization of the clay adsorbents (KBR, KBTA, and KBAA)

3.1.1. XRF analysis

An X-ray fluorescence spectrometer was used to determine the changes in the chemical composition of the clay before and after activation (Table 1). As can be observed from the table, the octahedral cations such as Al^{3+}, Fe^{3+}, and Mg^{2+} were reduced appreciably after the acid treatment, while the tetrahedral cation, like Si^{4+}, increased with acid treatment. The behavior shown by the Al_2O_3, Fe_2O_3, and MgO content with acid treatment is related to the progressive dissolution of the clay minerals. The octahedral sheet destruction passes the cations into the solution, while the silica generated by the tetrahedral sheet remains in the solids, due to its insolubility. Pesquera et al. [30] suggest that this free silica generated by the initial destruction of the tetrahedral sheet is polymerized by the effect of such high acid concentrations and is deposited on the undestroyed silicate fractions, protecting them from further attack. Apart from leaching out of the octahedral and tetrahedral cations, the acid activated samples showed a decrease in cation exchange capacity and an increase in surface area. The increase in surface area from the natural to thermal and acid activated samples could be related to the elimination of the exchangeable cations, delamination of the clay and the generation of microporosity during the process.

Table 1. X-ray fluorescence analysis of the clay samples.

Chemical constituents	Clay samples		
	KBR	KBTA	KBAA
Al_2O_3	25.78	25.82	2.63
SiO_2	52.65	55.66	89.59
Fe_2O_3	10.94	10.98	1.71
MgO	1.73	1.75	0.92
Na_2O	0.96	0.97	0.05
K_2O	0.61	0.62	0.01
CaO	1.13	1.14	0.05
TiO_2	2.41	2.42	1.28
LOI	4.79	0.53	3.34
Total	100	99.89	97.68
CEC (meq/100 g)	98	79	56
Surface area (m^2/g)	29.65	43.82	77.91
Si/[Al + Fe + Mg]	1.37	1.44	17.03

3.1.2. Thermal analysis

Figure 1 shows the differential thermal analysis (DTA) profile of the Kono-Bowe clay. The DTA of the clay was carried out to analyze the effect of heating on the surface and structural properties of the clay. The results reveal that the dehydration stage corresponding to the removal of adsorbed and hydrated water can be seen at 106.8 °C. This is the first endothermic peak. It could be seen that the maxima of the DTA curve occurs at 442.4 °C. The removal of adsorbed and hydrated water provides additional adsorption sites and an increase in surface area was observed. Further heating indicates the transition from dehydration stage to dehydroxylation stage. The second endothermic peak appears at 528.3 °C, showing the maximum breaking point at about 800 °C. Heating beyond these temperatures results in collapse of the interlayer spaces, and consequently rupture of the clay structure, which causes morphological changes and decrease in surface area at high temperatures.

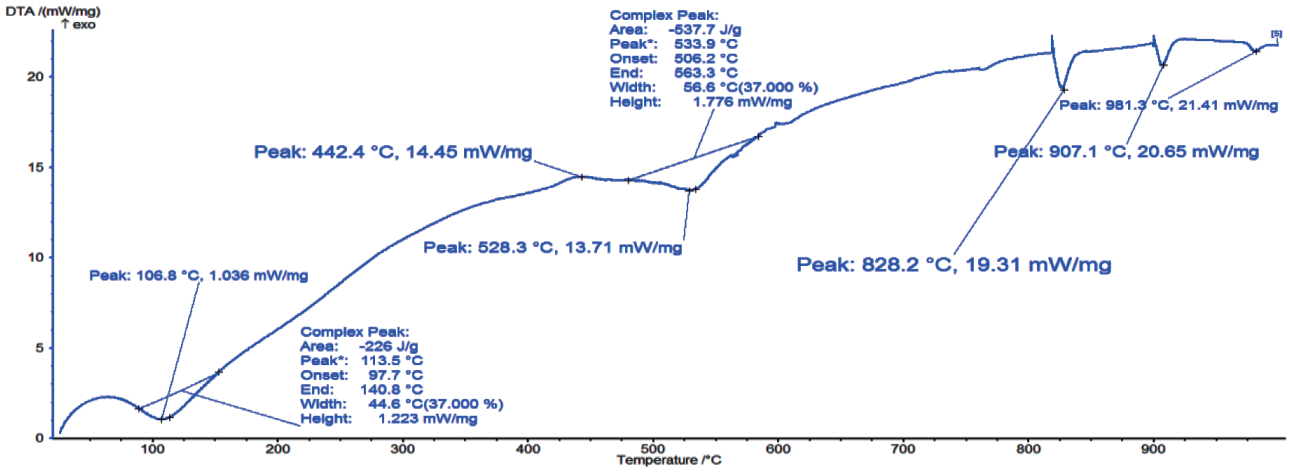

Figure 1. Differential thermal analysis profile of the raw Kono-Bowe clay.

3.1.3. X-ray diffraction analysis of the samples

The XRD patterns of raw, thermally activated, and acid activated bentonite are shown in Figures 2a, 2b, and 2c, respectively. Montmorillonite (M) was the main mineral; however, minor amounts of quartz (Q), chyrstoballitte (C), and calcium carbonate are present and these results are in accordance with the literature [31–33]. The strong diffraction peaks at $2\theta = 26.7°$ and $31.06°$ can be ascribed to the characteristic diffraction of quartz and chrystoballite impurities [34], respectively, which indicated the existence of quartz impurities. Moreover, the diffraction peaks at $2\theta = 21.6°$ and $36.4°$ reveal the presence of small amounts of calcites. After treatment with H_2SO_4 solution, the characteristic peaks of montmorillonite, calcium carbonate, and chrystoballite almost disappeared, indicating that these impurities were removed. The diffraction peaks at $2\theta = 7.45°$ are assigned to the (110) characteristic peaks of sepiolites [35,36].

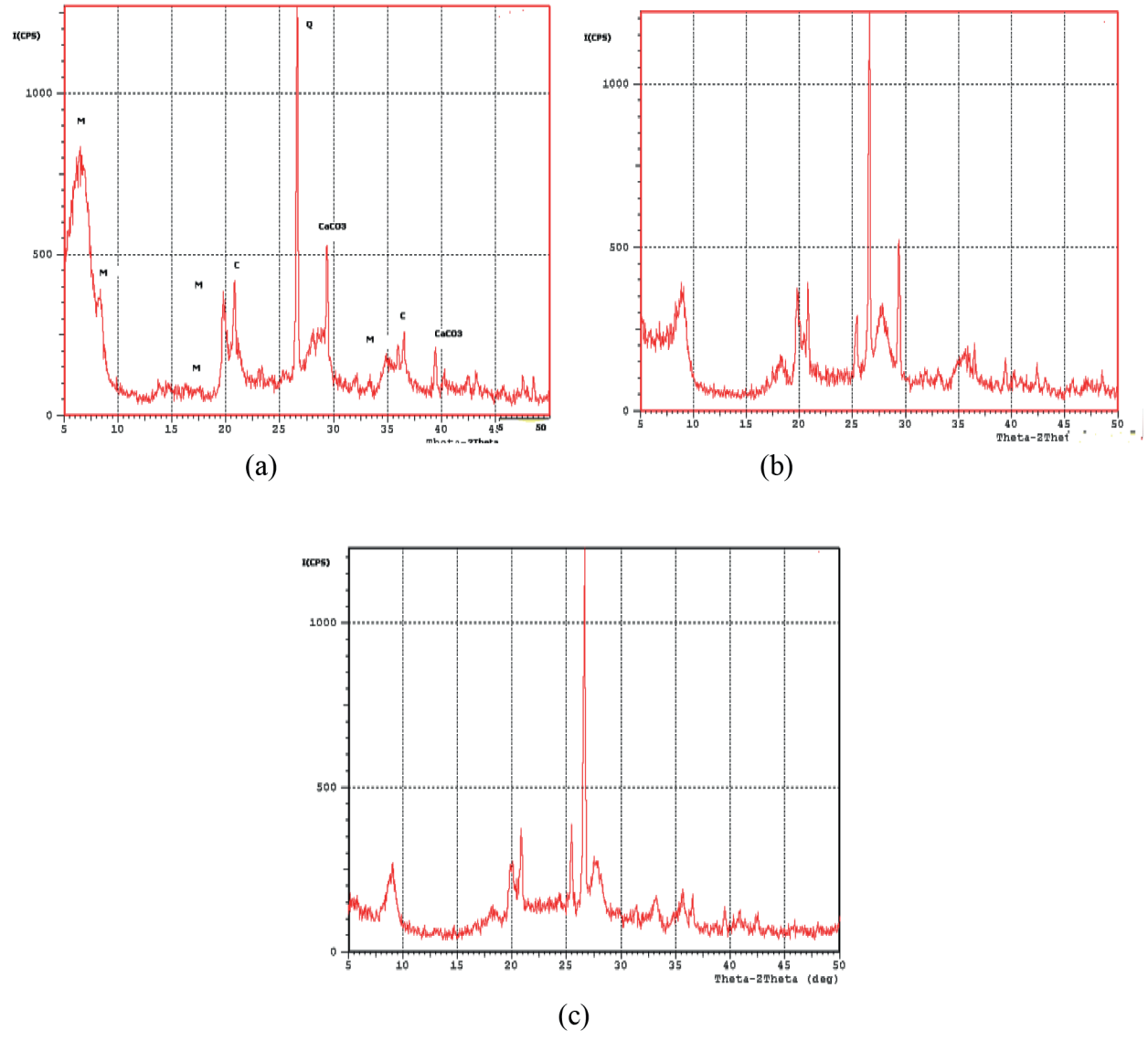

Figure 2. XRD patterns for the sorbent; (a) raw sample, (b) thermally activated sample, (c) sulfuric acid activated sample.

3.2. pH point of zero charge of the adsorbent

The point of zero charge (pH_{PZC}) is the pH at which the total number of positive and negative charges on its surface becomes zero. The pH at the point of zero charge (pH_{PZC}) of the adsorbents was measured by using the pH drift method [27]. It can be observed from Figure 3 that the surface charges of the adsorbents KBR, KBTA, and KBAA are 7.8, 7.2, and 6.8, respectively, where the ΔpH values are zero. It has been reported previously [37] that the pH_{pzc} of an adsorbent decreases with increase in acidic groups on the surface of the adsorbents. From the results, it can be concluded that acid modification of the adsorbent gave a positive (acidic) surface charge for the adsorbent since the pH_{pzc} for the modified surface was found to be lower than that of the unmodified surface. The relationship between pH_{pzc} and adsorption capacity is that cations adsorption on any adsorbent will be expected to increase at pH value higher than the pH_{pzc} while anions adsorption will be favorable at pH values lower than the pH_{pzc} [38]. According to the literature, the adsorption of cations is favored at pH $>$ pH_{PZC}, while the adsorption of anions is favored at pH $<$ pH_{PZC}. Thus, the determination of this parameter is significant for the assessment of the sorption mechanism and the probable sorbate/sorbent interactions.

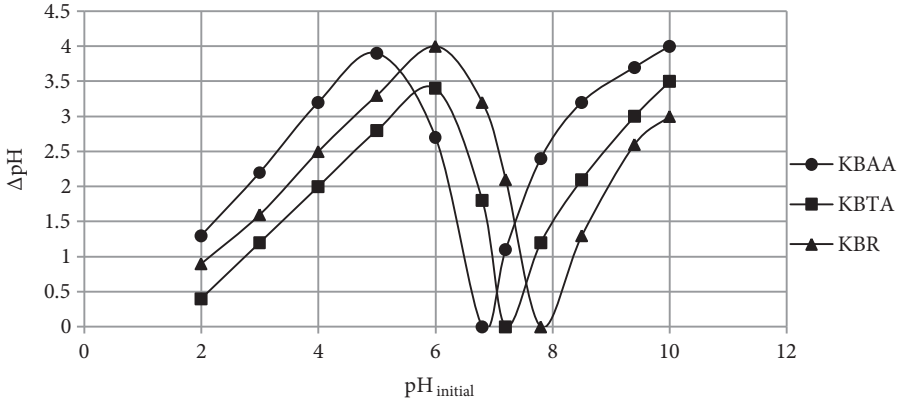

Figure 3. pH at the point of zero charge (pH_{PZC}).

3.3. Effect of process variables

3.3.1. Effect of pH on the sorption performance of the adsorbents

The effect of pH on the sorption performance of the adsorbents was studied in the range of 2 to 10 and the results are shown in Figures 4a and 4b for Pb(II) and Cr(III) removal, respectively. The adsorption patterns are similar, and the amount of metal uptake increases from almost zero to complete adsorption within a specific and fairly narrow pH range. Estimating the optimum pH for metal removal is vital since the pH of a solution affects the surface charge of the adsorbents, degree of ionization, and solution composition (metal speciation). Moreover, the level of dissociation of functional groups on the adsorbent surface, solubility of metal ions, and concentration of the counter ions in solution are affected by pH [38–40]. The decrease in uptake at higher and lower pH may be attributed to the formation of precipitates of the metal hydroxides at higher pH and formation of more H^+ ions at lower pH, which might compete with the metal ions for active sites on the adsorbent surface. According to Low et al. [41], at low pH values, the surface of the adsorbents would be closely associated with hydroxonium ions (H_3O^+), which might hinder the access of the metal ions, by repulsive forces, to the surface functional groups and consequently decrease the percentage metal removal. Therefore, the effect of low pH on

the sorption capacity may be interpreted to result from competition of the H_3O^+ and metal ions for binding sites. At low pH values, the ligands on the cell walls are closely associated with the hydroxonium ions, thereby causing the surface of the adsorbents to be positively charged, but when the pH is increased the hydroxonium ions are gradually dissociated and the positively charged metal ions are associated with the free binding sites on the adsorbent. This result also suggests that H+ ion concentration on these adsorbents affects the amount of metal ions adsorbed [42].

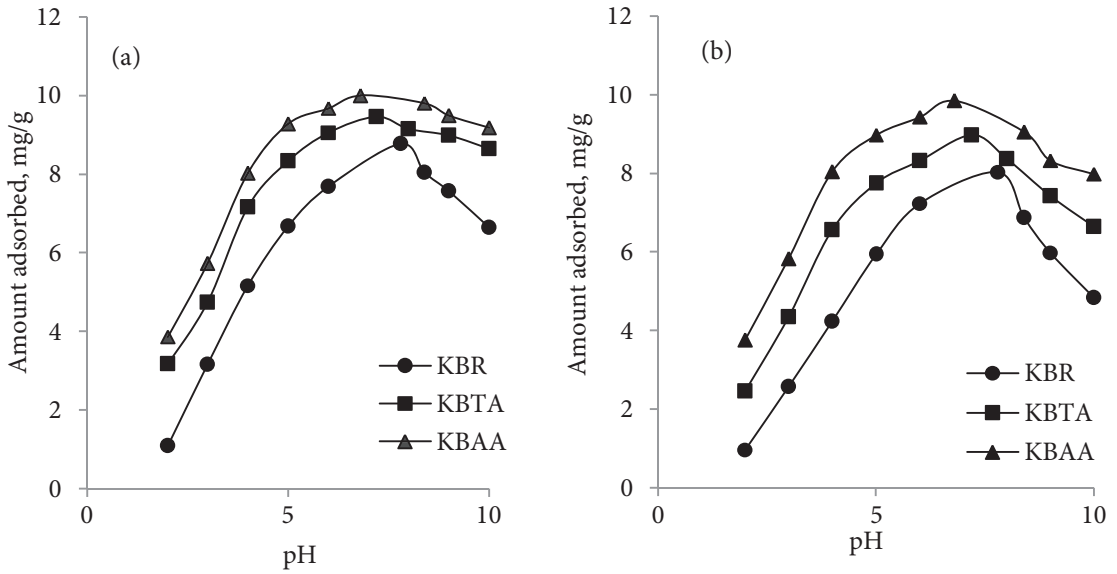

Figure 4. Effect of pH on the sorption performance of the clay sorbents, KBR, KBTA, and KBAA, for (a) Pb(II) and (b) Cr(III) removal from aqueous solutions.

3.3.2. Effect of contact time

The effect of contact time on the removal of Cr(III) and Pb(II) by raw and modified clay at initial metal ion concentrations of 100 mg/L is shown in Figures 5a and 5b, respectively. The contact time was varied from 15 to 270 min at constant temperature of 333 K. The time plot shows that the removal of adsorbate is rapid in early stages for the raw and modified clay, but it gradually slows down until it reaches the equilibrium. This is due to the fact that a large number of vacant surface sites are available for adsorption during the initial stage, and after a lapse of time the remaining vacant surface sites are difficult to be occupied due to repulsive forces between the solute molecules on the solid surface and in bulk phase [43]. From Figure 5b, which shows the adsorption of Cr(III), the equilibrium was attained after shaking for 120 min for KBAA, 180 min for KBTA, and 210 min for KBR, while in Figure 5a equilibrium was attained for Pb(II) removal after shaking for 180 min for KBAA, 210 min for KBTA, and 240 for KBR. Once equilibrium was attained, the percentage sorption of the metal ions did not change with further increases in time.

3.3.3. Effect of initial metal ion concentration

The effect of initial metal ion concentration on the adsorption performance of raw clay and clay modified by acid and thermal activation was investigated over a concentration range of 100 mg L^{-1} to 500 mg L^{-1}. The results of the experimental data are given in Figure 6 (a and b) for Cr(III) and Pb(II) removal, respectively. The adsorption capacity of the clay samples (KBR, KBTA, and KBAA) was found to increase with increase in initial

chromium and lead ions. The results show that sample KBAA gave the maximum adsorption of 40.72 mg g^{-1} and 34.66 mg g^{-1} at 500 mg L^{-1} of initial metal ion concentration for Cr(III) and Pb(II) removal, respectively. The adsorption capacity by the raw and modified clay follows the order KBAA > KBTA > KBR; and this indicates that there are more adsorption sites on KBAA than KBTA and KBR available for the adsorption of chromium and lead ions. The increase in adsorption with the increase in metal ion concentration is due to the driving force that initial concentration provides to overcome the mass transfer resistance between the aqueous and solid phases. The adsorption rate was high during the early adsorption period due to the availability of a large number of vacant sites, which increased the concentration gradient between the adsorbate in the solution and adsorbate on the adsorbent surface [44]. The steady increase in the adsorption with the increase in initial metal ion concentration indicates that the adsorbents have very high potential for the removal of lead(II) and chromium(III) ions.

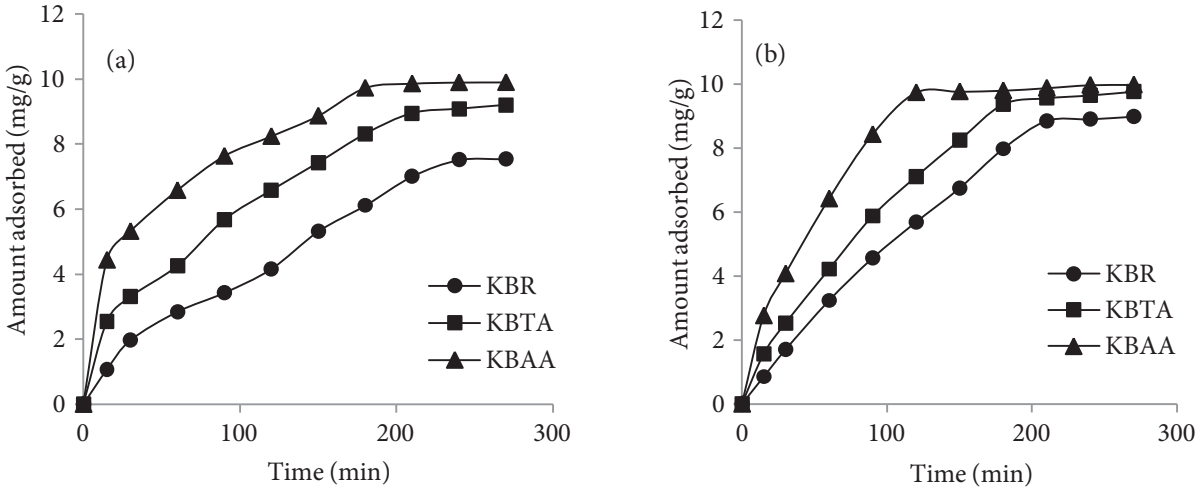

Figure 5. Effect of contact time on the sorption performance of the clay adsorbents for (a) Pb (II) and (b) Cr(III) removal from aqueous solutions.

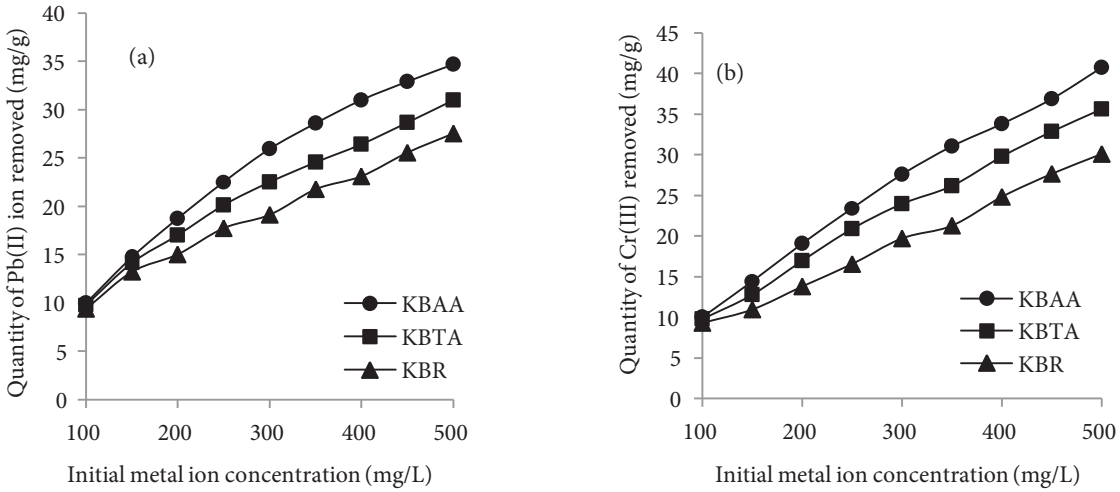

Figure 6. Effect of initial metal ion concentration on the sorption performance of the clay adsorbents for (a) Pb(II) and (b) Cr(III) ions' removal.

3.3.4. Effect of adsorbent dosage

The results of the effect of adsorbent dosage on the adsorption efficiency of the raw, thermal, and acid modified clay are shown in Figure 7 for Pb(II) and Cr(III) removal, respectively. It was observed from Figure 7 that the lead ion removal by the adsorbents increased as the adsorbent dosage increased gradually up to 3.5 g L^{-1} clay dosage. A further increase in dosage above 3.5 g L^{-1} gave no significant improvement in lead ion removal due to attainment of equilibrium between the adsorbent and adsorbate [45]. For chromium removal (Figure 8), equilibrium was achieved using the modified clay KBAA and KBTA at clay dosage of 3.0 g L^{-1}, while the KBR attained equilibrium at a dosage of 4.0 g L^{-1}. The increase in adsorption capacity of the raw and modified clay with increase in adsorbent dosage is attributed to the increase in surface area of micropores and the increase in availability of vacant adsorption sites [46].

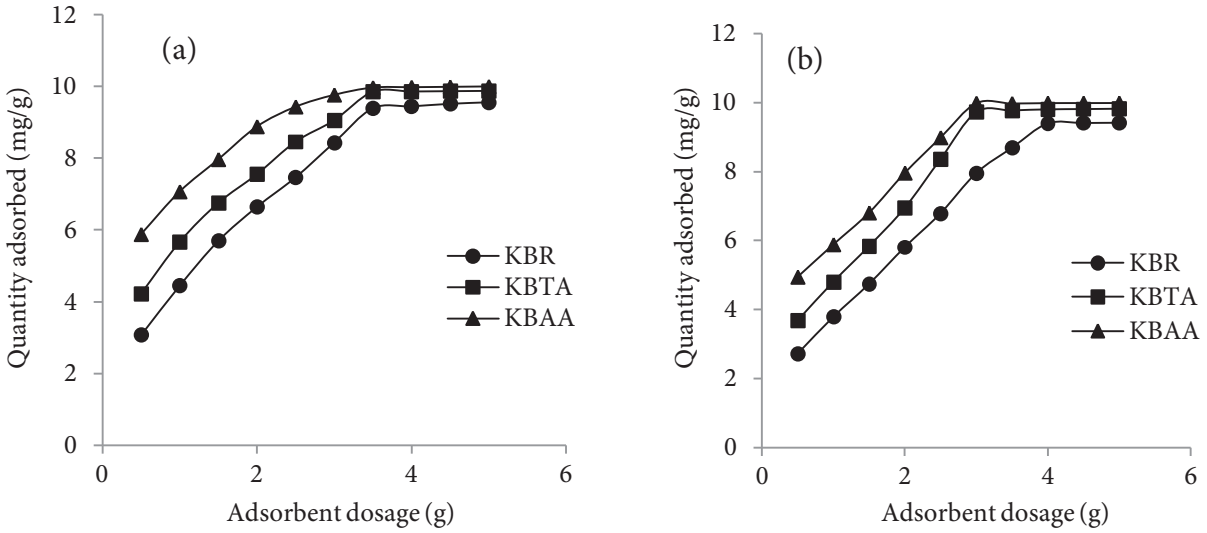

Figure 7. Effect of adsorbent dosage on the sorption performance of the clay sorbents for (a) Pb(II) and (b) Cr(III) ions' removal from aqueous solutions.

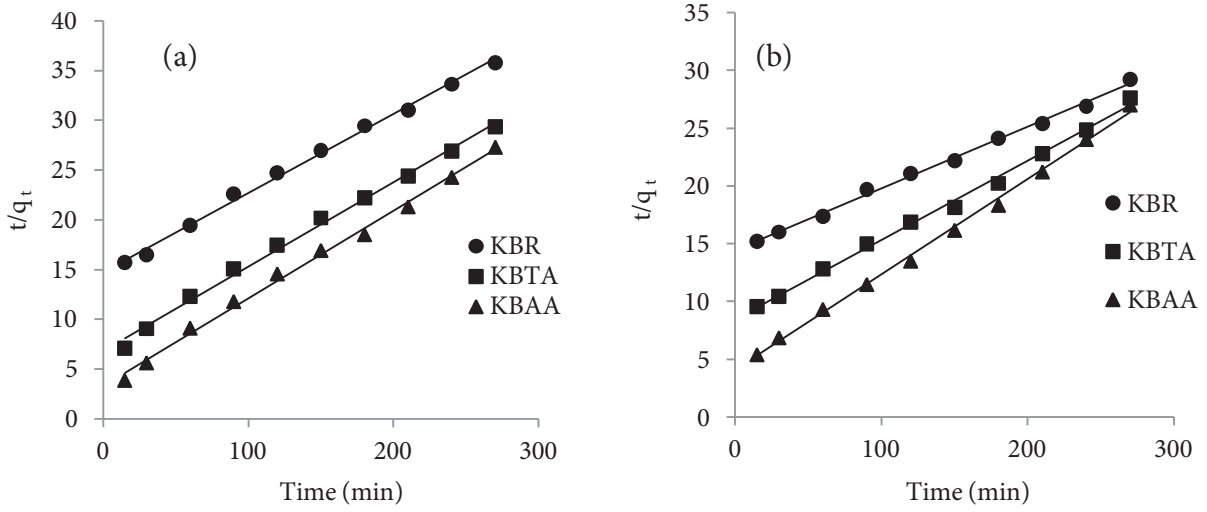

Figure 8. Pseudo-second-order kinetic plot for (a) Pb(II) and (b) Cr(III) adsorption onto clay sorbents.

3.4. Adsorption kinetics

The effect of contact time on the adsorption of Pb(II) and Cr(III) on raw and modified Kono-bowe clay was studied and the results show that adsorption increased with increase in contact time. The experimental data were examined by pseudo-first-order, pseudo-second-order, Elovich, Bangham, and intraparticle diffusion kinetic equations to understand the dynamics and mechanism of the adsorption process.

3.4.1. Pseudo-first-order kinetic model

A simple pseudo-first-order equation was used and it is given by

$$\frac{dq_t}{dt} = k_1 (q_e - q_t), \tag{3}$$

where q_e and q_t are the amount of metal ion adsorbed at equilibrium and at time t (min), respectively, and k_1 is the rate constant of the pseudo-first-order adsorption process [47,48]. The linear form of the equation is given as

$$\log (q_e - q_t) = \log q_e - \frac{k_1}{2.303} t \tag{4}$$

The values of k_1 and q_e were calculated from the slope and intercept of the linear plot of *log* $(q_e - q_t)$ versus t and are given in Table 2.

3.4.2. Pseudo-second-order kinetic model

The corresponding pseudo-second-order rate equation [49] is given as

$$\frac{t}{q_t} = \frac{1}{k_2 q_e^2} + \frac{t}{q_e}, \tag{5}$$

where k_2 is the rate constant for the pseudo-second order adsorption process (g mg^{-1} min^{-1}). The slope and intercept of the plot of t/q_t versus t for Pb(II) and Cr(III) removal (Figure 8) were used to calculate the values of q_e and k_2 as presented in Table 2. The value of the regression coefficient calculated from the plot of the second-order kinetic plot shows that it best fitted the experimental data and can be used to describe the adsorption of Pb(II) and Cr(III) onto raw and modified Kono-bowe clay.

3.4.3. Elovich kinetic model

The Elovich model is presented by the following equation:

$$q_t = \frac{1}{\beta} \ln \alpha\beta + \frac{1}{\beta} \ln t, \tag{6}$$

where α is the initial adsorption rate (mg/g/min) and β is the desorption constant (g/mg). The slope and intercept of the plot of q_t versus $ln\ t$ were used to calculate the values of the constants α and β as shown in Table 2. The values of the determination coefficient obtained from the linear plot of Elovich models are not high ($R^2 < 0.979$), suggesting that the applicability of this model to describe the adsorption process of Pb(II) and Cr(III) onto raw and modified Kono-bowe clay is not feasible.

Table 2. Parameters of the pseudo-first-order, pseudo-second-order, Elovich, Bangham, and intraparticle kinetic models together with their regression coefficients.

Kinetic models	Parameters	Pb(II)			Cr(III)		
		Sorbent samples					
		KBR	KBTA	KBAA	KBR	KBTA	KBAA
Pseudo-first-order	k_1 (min^{-1})	1.84×10^{-2}	9.21×10^{-3}	2.76×10^{-2}	1.84×10^{-2}	1.84×10^{-2}	2.53×10^{-2}
	q_e (mg/g)	3.320	2.694	3.597	19.409	16.788	13.428
	R_1^2	0.727	0.978	0.868	0.866	0.947	0.938
Pseudo-second-order	k_2 (g/mg min)	4.23×10^{-4}	1.03×10^{-3}	2.28×10^{-3}	1.95×10^{-4}	5.46×10^{-4}	1.64×10^{-3}
	q_e (mg/g)	12.658	11.905	11.494	18.868	14.706	12.195
	R_2^2	0.996	0.995	0.995	0.996	0.996	0.997
Elovich	B	0.426	0.392	0.989	0.319	0.312	0.361
	α (mg/g min)	0.1796	0.3287	0.8005	0.1960	0.2662	0.5108
	R_E^2	0.968	0.974	0.989	0.950	0.966	0.944
Bangham	k_0 (mol/g)	$6.6\ 0 \times 10^{-4}$	2.38×10^{-3}	7.40×10^{-3}	3.68×10^{-4}	1.02×10^{-3}	3.71×10^{-3}
	σ	0.774	0.592	0.411	0.936	0.774	0.557
	R_B^2	0.995	0.995	0.988	0.994	0.989	0.934
Intraparticle	K_{id} (mg/g $min^{0.5}$)	0.532	0.569	0.490	0.713	0.718	0.589
	C	–1.052	0.300	2.621	–2.064	–1.076	1.631
	R_i^2	0.998	0.987	0.988	0.986	0.972	0.985

3.4.4. Bangham's equation

Bangham's model [50] tests if pore diffusion is the only rate controlling step of an adsorption process. The model can be represented by the following equation:

$$\log\left[\log\left(\frac{c_0}{c_0 - q_t m}\right)\right] = \log\left(\frac{k_0 m}{2.303V}\right) + \sigma \log t, \tag{7}$$

where c_o, mg/L, is the initial sorbate concentration in the liquid phase; q_t, mg/g – sorbate concentration in the solid phase at time t, min; m, g/L – adsorbent concentration; V, L – solution volume; k_o, L/g, and $\sigma(\sigma < 1)$ – Bangham's equation parameters. The values of the constants were calculated from the slope and intercept of the plot of $log[log(c_o/(c_o - q_t m))]$ versus $log\ t$ and are shown in Table 2.

3.4.5. Intraparticle diffusion study

The adsorption mechanism of adsorbate onto adsorbent follows three steps: (1) transport of adsorbate from the boundary film to the external surface of the adsorbate; (2) adsorption at a site on the surface; (3) intraparticle diffusion of the adsorbate molecules to an adsorption site by a pore diffusion process. The slowest of the three steps controls the overall rate of the process. The possibility of intraparticle diffusion was explored by using an intraparticle diffusion model. The intraparticle diffusion varies with the square root of time and is given [49,51] as

$$q_t = k_{id} t^{1/2} + C_i, \tag{8}$$

where q_t is the amount adsorbed at time t, $t^{1/2}$ is the square root of the time, k_{id} is the intraparticle diffusion rate constant (mg/g $\text{min}^{1/2}$), and C_i is the intercept at stage i and is related to the thickness of the boundary layer. Large C_i represents the greater effect of the boundary layer on molecule diffusion. The intraparticle diffusion rate constant was determined from the slope of the linear gradients of the plot of q_t versus $t^{1/2}$ for Pb(II) and Cr(III) removal as shown in Figure 9; their values are presented in Table 2. The intraparticle diffusion process is controlled by the diffusion of ions within the adsorbent.

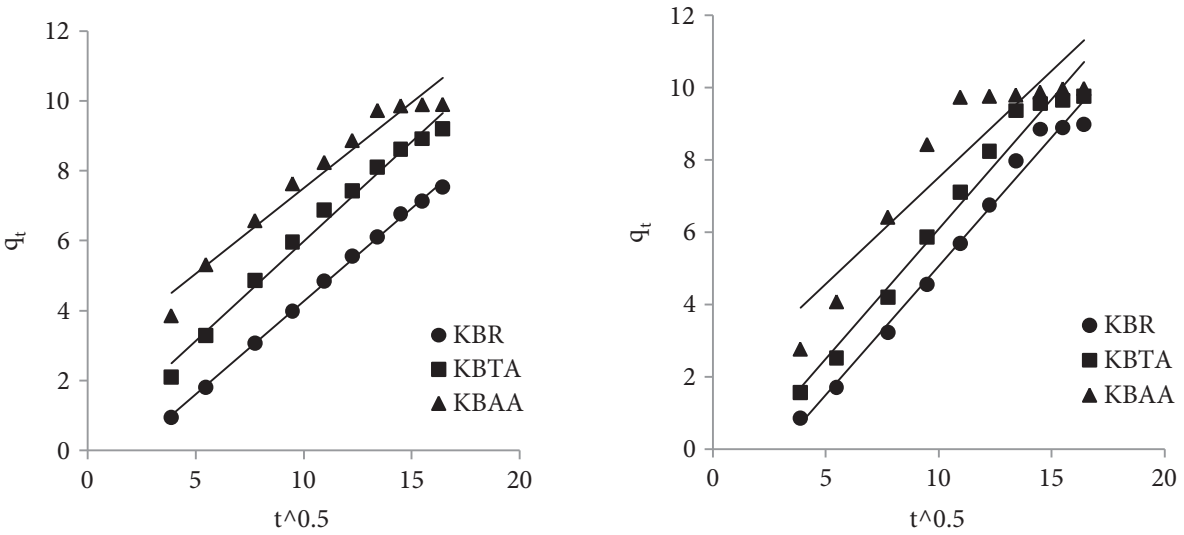

Figure 9. Plot of the intraparticle kinetic model for (a) Pb(II) and (b) Cr(III) adsorption onto clay adsorbents.

The plots of q_t against $t^{1/2}$ for the intraparticle diffusion model gave straight lines that do not pass through the origin (i.e. the intercepts > 0) (Figure 9). The deviation of these lines from the origin indicates that intraparticle diffusion may be a factor in the sorption process, but it is not the only controlling step [52]. The rate constants, ki, and boundary layer thickness, Xi, obtained from the model for the various adsorption systems studied are given in Table 2. The intercepts of the plots are an indication of the level of contribution of boundary layer resistance as it affects the rate limiting step of the sorption process. The larger the intercept, the greater is the contribution of the surface sorption (boundary layer resistance) in the rate-limiting step [53].

The commensurable and relatively high values of R_B^2 and R_i^2 for both studied systems, calculated by the Bangham's and the intraparticle diffusion models, proved the significant role of intraparticle diffusion as one of the probable rate controlling mechanisms during Pb(II) and Cr(III) adsorption on raw and modified Kono-bowe clay.

3.5. Adsorption isotherm

Equilibrium study on adsorption provides information on the capacity of the adsorbent. An adsorption isotherm is characterized by certain constant values, which express the surface properties and affinity of the adsorbent, and could also be used to compare the adsorptive capacities of the adsorbent for different pollutants. The adsorption isotherms of Pb(II) and Cr(III) onto KBR, KBTA, and KBAA were studied and the equilibrium data analyzed using Langmuir, Freundlich, Temkin, Dubinin–Radushkevich, and Harkin–Jura models.

3.6. Langmuir isotherm

The Langmuir isotherm model is based on the fact that uptake of metal ions occurs on a homogeneous surface by monolayer adsorption with no interaction between adsorbed molecules, with homogeneous binding sites, equivalent sorption energies, and no interaction between adsorbed species. The model is given by the following linear equation:

$$\frac{C_e}{q_e} = \frac{1}{q_m K_L} + \frac{C_e}{q_m}, \tag{9}$$

where C_e is the equilibrium concentration (mg/L), q_e is the amount of metal ion adsorbed (mg/g), q_m is the Langmuir constant for adsorption capacity (mg/g), and K_L is sorption equilibrium constant (L/g).

The values of q_m and K_L were evaluated from the slope and intercept of the plot of C_e/q_e versus C_e as shown in Figure 10 [54,55] and are given in Table 3. From the values of the determination coefficient in Table 3, it can be seen that the Langmuir isotherm fitted the data for the sorption activities of the sorbent KBR for both Pb(II) and Cr(III), while the other sorbents did not fit.

A further analysis of the Langmuir equation can be made on the basis of a dimensionless equilibrium parameter, R_L [56], also known as the separation factor, and has been suggested to express the essential characteristics of the Langmuir isotherm [57–59]. It is a measure of the favorability of the adsorption process [60]. R_L is given by

$$R_L = \frac{1}{(1 + K_L C_0)} \tag{10}$$

The value of R_L lies between 0 and 1 for favorable adsorption, while $R_L > 1$ represents unfavorable adsorption and $R_L = 1$ represents linear adsorption while the adsorption process is irreversible if $R_L = 0$. Results of R_L

Table 3. Langmuir, Freundlich, Temkin, Dubinin–Radushkevich, and Harkin–Jura isotherm parameters for adsorption of Pb(II) and Cr(III) on to KBR, KBTA, and KBAA.

Isotherm models	Parameters	Clay samples					
		Pb(II)			Cr(III)		
		KBR	KBTA	KBAA	KBR	KBTA	KBAA
Langmuir	q_m (mg/g)	34.48	32.26	35.71	40.00	41.67	43.48
	K_L(L/mg)	1.466×10^{-2}	5.032×10^{-2}	10.33×10^{-2}	1.293×10^{-2}	2.791×10^{-2}	9.663×10^{-2}
	R^2	0.9978	0.9762	0.987	0.9957	0.9096	0.9780
Freundlich	K_f (mg/g)	2.133	6.561	11.220	2.004	3.097	8.531
	n	2.096	3.50	4.55	2.024	2.049	2.809
	R^2	0.9694	0.997	0.995	0.9782	0.9958	0.9979
Temkin	B_1	4.619	4.328	3.915	7.525	8.622	7.902
	K_T	1.108	3.151	21.880	0.160	0.297	1.342
	R^2	0.8992	0.9294	0.9307	0.827	0.913	0.978
Dubinin–Radushkevich	X_m(mg/g)	8.74	10.79	12.99	6.639	8.837	12.554
	β ($\times 10^{-9}$)	–4.950	–4.966	–5.485	–6.584	–7.329	–7.974
	E (kJ/mol)	–10.050	–10.034	–9.548	–8.714	–8.259	–7.918
	R^2	0.9811	0.9748	0.9060	0.9359	0.9679	0.9150
Harkin–Jura	A	200	250	333.33	142.86	125	250
	B	2.8	2.5	2.33	2.57	2.125	2.25
	R^2	0.9431	0.9335	0.9334	0.9817	0.8632	0.8348

calculated from this study (shown in Figure 11) lie between 0.019 and 0.436 and this is consistent with the requirement for favorable adsorption of Pb(II) and Cr(III) onto KBR, KBTA, and KBAA.

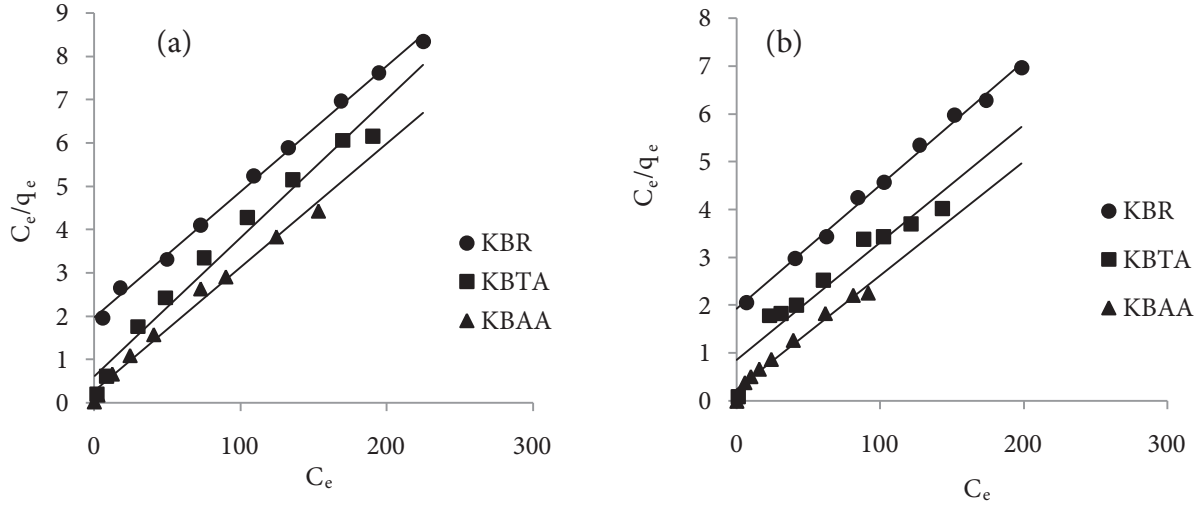

Figure 10. Langmuir isotherm plot for (a) Pb(II) and (b) Cr(III) adsorption onto clay sorbents.

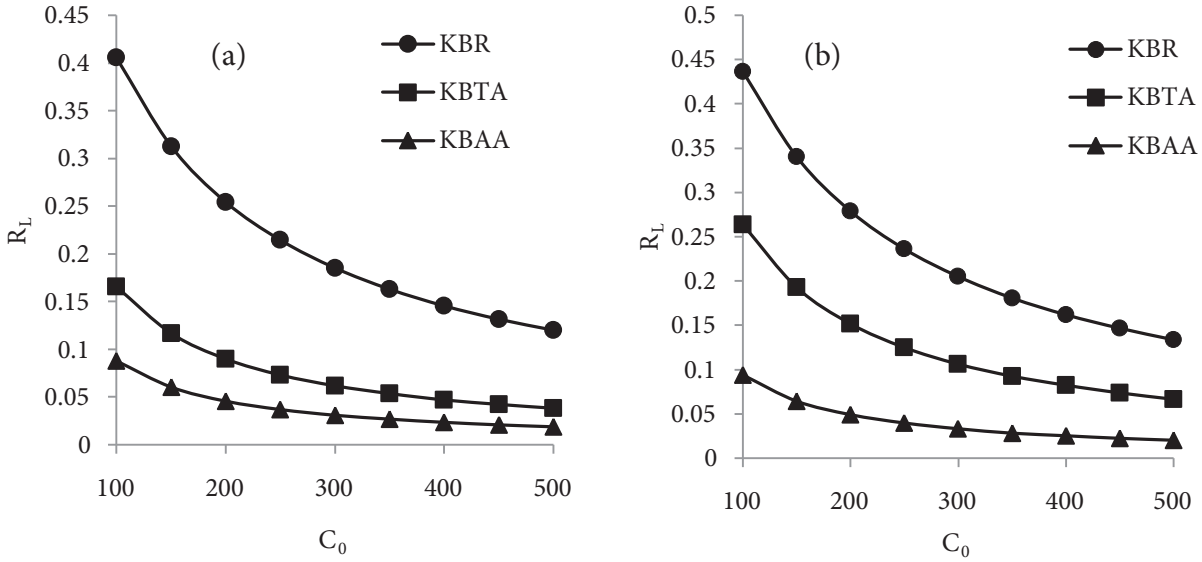

Figure 11. Plot of separation factor, R_L, versus C_0, (a) Pb(II) (b) Cr(III).

3.6.1. Freundlich isotherm

The Freundlich isotherm assumes that the uptakes of metal ions occur on a heterogeneous surface by multilayer adsorption and that the amount of adsorbate adsorbed increases infinitely with an increase in concentration. It is a very popular model for a single solute system, based on the distribution of solute between the solid phase and aqueous phase at equilibrium [61]. The Freundlich equation is expressed as

$$q_e = K_f C_e^{1/n}, \tag{11}$$

where K_f is the measure of adsorption capacity and n is the adsorption intensity. The linear form of the Freundlich equation [62] is

$$\log q_e = \log K_f + \frac{1}{n} \log C_e, \tag{12}$$

where q_e is the amount adsorbed (mg/g), C_e is the equilibrium concentration of adsorbate (mg/L), and K_f and n are the Freundlich constants related to the adsorption capacity and adsorption intensity, respectively. A plot of *log* q_e vs. *log* C_e (Figures 12a and 12b) gives a linear trace with a slope of *1/n* and intercept of *log* K_f and the results are also given in Table 3. When *1/n* >1.0, the change in adsorbed metal ion concentration is greater than the change in the metal ion concentration in solution. While the Langmuir isotherm model gave the best description of Pb(II) and Cr(III) adsorption in KBR, the Freundlich equation was the most suitable model for describing the Pb(II) and Cr(III) adsorption in KBTA and KBAA. This is evident from the high regression factor obtained for the sorption processes (Table 3). The Langmuir isotherm makes an assumption that the adsorption occurs at specific homogeneous sites within the adsorbent [63,64]. From the Freundlich isotherm, since the values of 1/n < 1 in all the sorption processes studied, then the adsorption was favorable and the adsorption capacity increased with the occurrence of new adsorption sites [65]. These values also satisfy the condition for heterogeneity, i.e. 1 < n < 10 [66].

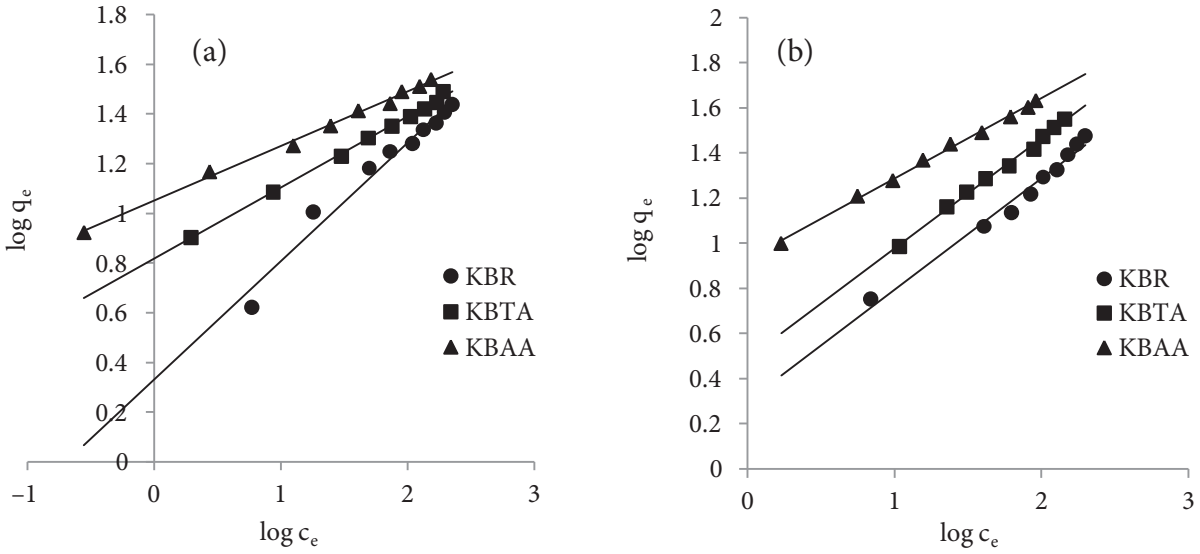

Figure 12. Freundlich isotherm plot for (a) Pb(II) and (b) Cr(III) adsorption onto clay sorbents.

3.6.2. Temkin isotherm model

The Temkin isotherm model [67] has been developed on the concept of chemisorptions and assumes that the heat of adsorption of the sorbate molecules decreases linearly with adsorbent layer coverage due to adsorbate–adsorbent interactions. The equation and its linearized form are represented as follows:

$$q_e = \frac{RT}{b_T} \ln (K_T C_e) \tag{13}$$

$$q_e = B_1 \ln K_T + B_1 \ln C_e, \tag{14}$$

where $B_1 = RT/b_T; b_T$, $mol\ kJ^{-1}$, is the Temkin isotherm constant; K_T, mol g^{-1}, is the equilibrium binding constant; T, K, the temperature and $R(8.314 \times 10^{-3}$ kJ mol^{-1} $K^{-1})$ the universal gas constant. The isotherm parameters, B_1 and K_T, were calculated from the slope and intercept of the linear plot of q_e vs. ln C_e and their values are listed in Table 3. The correlation coefficients obtained from this plot were high (>0.913) for Pb(II) and Cr(III) adsorption on KBTA and KBAA. This suggests that there was a sort of interaction between the molecules of the metal and adsorbent as the isotherm takes into account the effects of indirect adsorbate/adsorbent interactions on the adsorption process.

3.6.3. Dubinin–Radushkevich isotherm

The D-R equation has been widely used to explain energetic heterogeneity of solid at low coverage as monolayer regions in micropores. The equation is given by

$$\ln q_e = \ln X_m - \beta\varepsilon^2, \tag{15}$$

where β is the activity coefficient related to mean adsorption energy, X_m the maximum of adsorption capacity, and ε the Polangi potential, which is equal to

$$\varepsilon = RT \ln\left(\frac{1}{C_e}\right), \tag{16}$$

where R and T are the gas constant (kJ/mol/K) and temperature (K), respectively.

The adsorption energy E expressed as

$$E = -\frac{1}{(-2\beta)^{0.5}} \tag{17}$$

reveals the nature of adsorption. If the value of adsorption energy E ranged between –1 and –8 kJ/mol, the adsorption process is physical, and if the value of E ranged between –9 and –16 kJ/mol, it is chemical adsorption. The parameters of the D-R equation were calculated from the slope and intercept of the linear plot of $\ln q_e$ versus ε^2 and are given in Table 3.

The adsorption energy E value obtained in the range of –9 kJ/mol to –10.00 kJ/mol for Pb(II) adsorption on all the adsorbents showed that the adsorption is a chemical process, while the E value in the range of –7 kJ/mol to –8 kJ/mol for Cr(III) adsorption onto all the studied sorbents showed physical adsorption.

3.6.4. Harkin–Jura isotherm

The Harkin–Jura isotherm model takes into consideration the multilayer adsorption, which can be explained by the existence of heterogeneous pore distribution. The equation is [68,69]

$$\frac{1}{q_e^2} = \left(\frac{B}{A}\right) - \left(\frac{1}{A}\right) logc_e \tag{18}$$

Comparing the values of the determination coefficient in Table 3, it can be seen that the adsorption of Pb(II) and Cr(III) on raw and modified clay sorbents from Kono-bowe cannot be described by this isotherm model.

The good fit of the experimental data and the determination coefficient closer to unity indicated the applicability of the Freundlich isotherm model to describe the adsorption of Pb(II) and Cr(III) onto KBTA and KBAA.

3.7. Adsorption thermodynamics

The thermodynamics of an adsorption process is obtained from a study of the influence of temperature on the process. Temperature effect was studied for the adsorption of Pb(II) and Cr(III) ions by KBR, KBTA, and KBAA. It was found that the adsorption capacity of KBR, KBTA, and KBAA for Pb(II) increased from 1.945 mg/g to 9.145 mg/g, 3.278 mg/g to 9.674 mg/g, and 4.976 mg/g to 9.972 mg/g, respectively, while for Cr(III) the adsorption capacity increased from 2.009 mg/g to 9.023 mg/g, 3.741 mg/g to 9.715 mg/g, and 5.649 mg/g to 9.999 mg/g, respectively (Figures 13a and 13b) as the temperature was increased from 303 K to 333 K at initial ion concentration of 100 mg/L. This indicates that the adsorption reaction was endothermic in nature. The enhancement in the adsorption capacity may be due to the chemical interaction between adsorbate and adsorbent, creation of some new adsorption sites, or the increased rate of intraparticle diffusion of Pb(II) and Cr(III) ions into the pores of the adsorbent at higher temperatures [51].

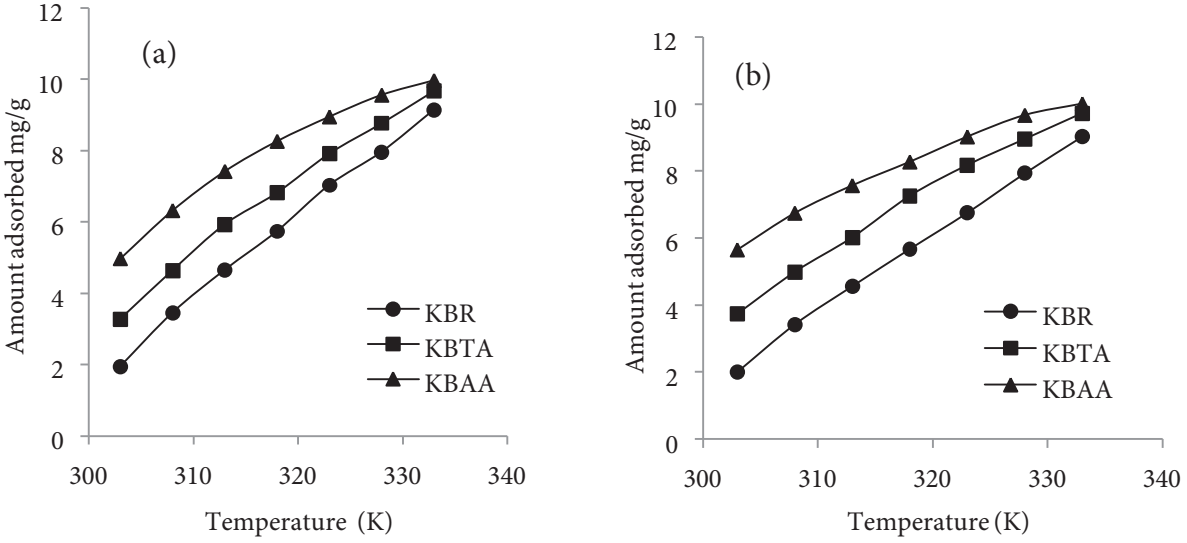

Figure 13. Effect of temperature on the sorption performance of the clay adsorbents for (a) Pb(II) and (b) Cr(III) ions' removal from aqueous solutions.

The standard Gibbs energy was

$$\Delta G^{\circ} = -RT \ln K_c \tag{19}$$

K_c represents the ability of the adsorbent to retain the adsorbate and the extent of movement of the adsorbate within the solution [70]. The values of K_c can be deduced from the relationship

$$K_c = \frac{q_e}{C_e}, \tag{20}$$

where q_e is the amount adsorbed on solid phase at equilibrium and C_e is the equilibrium concentration of metal ion in the solution. Other thermodynamic parameters such as change in standard enthalpy (ΔH°) and standard entropy (ΔS°) were determined using the Van't Hoff equation [6]

$$\ln K_c = \frac{\Delta S}{R} - \frac{\Delta H}{RT} \tag{21}$$

The values of ΔH° and ΔS° were obtained from the slope and intercept of the Van't Hoff plot of $\ln k_c$ versus *1/T* as shown in Figures 14a and 14b. A positive value of ΔH° indicates that the adsorption process is endothermic and this suggests that the total energy absorbed in bond breaking is greater than the total energy released in bond making between adsorbate and adsorbent, resulting in the absorption of extra energy in the form of heat. The magnitude of ΔH also shows the type of sorption; for physical adsorption, the magnitude falls into the range of 2.1–20.9 kJ/mol while that of chemisorptions generally falls into the range of 80–200 kJ/mol. Considering the values of ΔH calculated in this work, it can be deduced that the sorption of Pb(II) and Cr(III) onto raw and modified clay from Kono-bowe is a pure chemical adsorption process. The negative values of ΔG° reflect the feasibility of the process and the values become more negative with increase in temperature, which implies that lower temperature makes the adsorption easier for all the adsorbents. Standard entropy determines the disorderliness of the adsorption at the solid–liquid interface. Thermodynamic parameters are summarized in Table 4. The positive value of ΔS° shows increasing randomness at the solid–liquid interface with some structural changes in the adsorbate and adsorbent during the adsorption of both Pb(II) and Cr(III) ions on raw and modified Kono-bowe clay. The adsorbed solvent molecules gain more translational entropy than is lost by the adsorbate ions/molecules, thus allowing for the prevalence of randomness in the system.

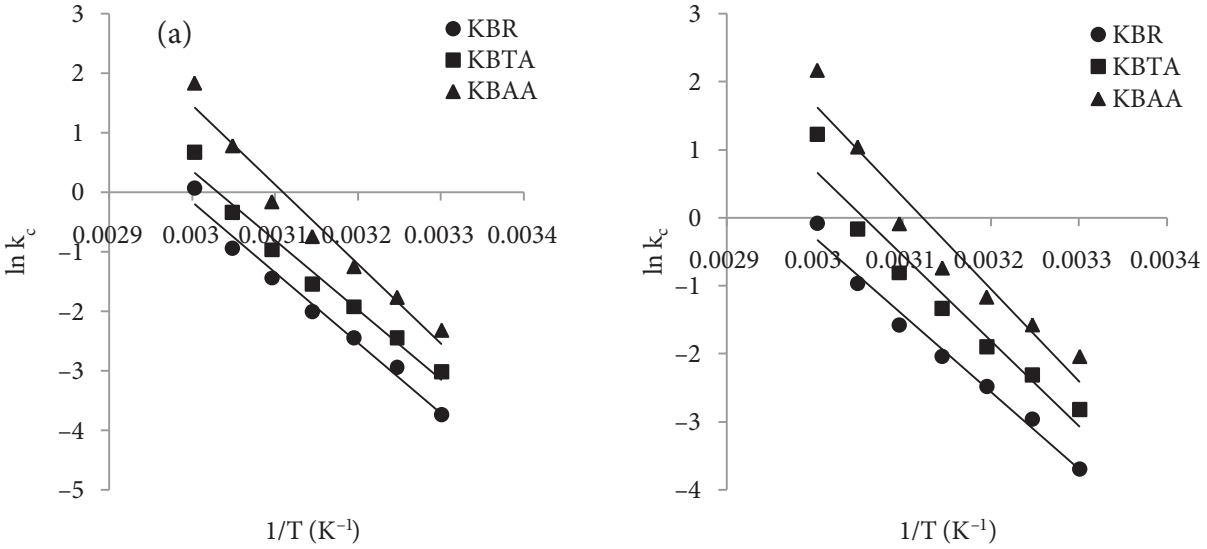

Figure 14. Plot of ln k_c versus T^{-1} for (a) Pb(II) and (b) Cr(III) adsorption.

4. Conclusions

This study shows that clay from Kono-bowe has great potential as adsorbent usable for the sorption of Pb(II) and Cr(III) ions from aqueous solutions. The amounts of Pb(II) and Cr(III) ions adsorbed are temperature, initial ion concentration, pH, contact time, and adsorbent dosage dependent. Langmuir, Freundlich, Temkin, Harkin–Jura, and DKR models describe the adsorption isotherm but the best fit ($R^2 = 0.99$) of experimental data is obtained with the Langmuir isotherm for KBR, while Freundlich gave best fit ($R^2 = 0.99$) for KBTA and KBAA sorbents. The adsorption process is spontaneous because of negative Gibbs free energy values given. It is accompanied by an exothermic interaction and positive values of ΔS^0 change. The adsorption obeys the pseudo-second-order kinetic model and is controlled by a chemical mechanism.

Table 4. Thermodynamic parameters for the removal of Pb(II) and Cr(III) ions from aqueous solutions using raw and modified Kono-bowe clay.

Temperature (K)	Pb(II) removal								
	KBR			KBTA			KBAA		
	ΔH (kJ/mol)	ΔS (J/mol)	ΔG (kJ/mol)	ΔH (kJ/mol)	ΔS (J/mol)	ΔG (kJ/mol)	ΔH (kJ/mol)	ΔS (J/mol)	ΔG (kJ/mol)
303	98.105	29	–8.884	96.983	28.6	–8.571	111.066	33.5	–10.258
308			–9.029			–8.903			–10.426
313			–9.174			–9.046			–10.593
318			–9.319			–9.189			–10.761
323			–9.464			–9.332			–10.928
328			–9.609			–9.475			–11.096
333			–9.754			–9.618			–11.263
Cr(III) removal									
303	94.098	28	–8.578	104.19	31.8	–9.740	112.66	35.2	–10.778
308			–8.718			–9.899			–10.954
313			–8.858			–10.058			–11.130
318			–8.998			–10.217			–11.306
323			–9.138			–10.376			–11.482
328			–9.278			–10.535			–11.658
333			–9.418			–10.694			–11.834

References

[1] Gholami F, Mahvi AH, Omrani GA, Nazmara S, Ghasri A. Removal of chromium (VI) from aqueous solution by ulmus leaves. Iran J Environ Health Sci Eng 2006; 3: 97-102.

[2] Olayinka KO, Alo BI, Adu T. Sorption of heavy metals from electroplating effluents by low cost adsorbents II: use of waste tea, coconut shell and coconut husk. J Appl Sci 2007; 7: 2307-2313.

[3] Bhatti I, Qureshi K, Kazi RA, Ansari AK. Preparation and characterization of chemically activated almond shells by optimization of adsorption parameters for removal of chromium VI from aqueous solutions. World Acad Sci Eng Technol 2007; 34: 199-204.

[4] Sarin V, Pant KK. Removal of chromium from industrial waste by using eucalyptus bark. Bioresource Technol 2006; 97: 15-20.

[5] Demirbas E, Kobyab M, Senturk E, Ozkan T. Adsorption kinetics for the removal of chromium (VI) from aqueous solutions on the activated carbons prepared from agricultural wastes. Water S A 2004; 30: 533-540.

[6] Demiral H, Demiral I, Tumsek F, Karabacakoglu B. Adsorption of chromium (VI) from aqueous solution by activated carbon derived from olive bagasse and applicability of different adsorption models. Chem Eng J 2008; 144: 188-196.

[7] Bhattacharyya KG, Sharma A. Kinetics and thermodynamics of Methylene Blue adsorption on Neem (*Azadirachta indica*) leaf powder. Dyes Pig 2005; 65: 51-59.

[8] Bhattacharyya KG, Gupta S. Adsorption of chromium (VI) from water by clays. Ind Eng Chem Res 2006; 45: 7232-7240.

[9] Gode F, Ozturk N, Sert Y, Bahceli S. Adsorption of Cr(VI) from aqueous solutions onto raw and acid-activated resadiye and hancili clays. Spectroscopy Let 2010; 43: 68-78.

[10] Arfaoui S, Frini-Srasra N, Srasra E. Modelling of the adsorption of the chromium ion by modified clays. Desalination 2008; 222: 474-481.

[11] Sharma YC, Weng CH. Removal of chromium (VI) from water and wastewater by using riverbed sand: kinetic and equilibrium studies. J Hazard Mater 2007; 142: 449-454.

[12] Katsumata H, Kaneco S, Inomata K, Itoh K, Funasaka K, Masuyama R, Suzuki T, Ohta K. Removal of heavy metals in rinsing wastewater from plating factory by adsorption with economical viable materials. J Environ Manage 2003; 69: 187-191.

[13] Gang D, Banerji SK, Clevenger TE. Factors affecting chromium (VI) removal by modified poly(4-vinylpyridine) coated silica gel. Practice Periodical of Hazard, Toxic, Radioactive Waste Management 2001; 5: 58-65.

[14] Chowdhury P, Mondal P, Roy K. Synthesis of polyaniline nanoparticle grafted silica gel and study of its Cr(VI) binding property. J Appl Poly Sci 2011; 119: 823-829.

[15] Chowdhury P, Mondal P, Roy K. Synthesis of cross-linked graft copolymer from [2-(methacryloyloxy)ethyl] trimethylammonium chloride and poly(vinyl alcohol) for removing chromium(VI) from aqueous solution. Poly Bull 2010; 64: 351-362.

[16] Khan SA, Rehman R, Khan MA. Adsorption of chromium (II), chromium (VI) and silver (I) on bentonite. Waste Manage 1995; 15: 271-282.

[17] Donat R, Akdogan A, Erdem E, Cetisli H. Thermodynamics of Pb^{2+} and Ni^{2+} adsorption onto natural bentonite from aqueous solutions. J Colloid Interface Sci 2005; 286: 43-52.

[18] Brigatti MF, Lugli C, Poppi L. Kinetics of heavy metal removal and recovery in sepiolite. Appl Clay Sci 2000; 16: 45-57.

[19] Brigatti MF, Medici L, Poppi L. Sepiolite and industrial waste water purification: removal of Zn^{2+} and Pb^{2+} from aqueous solutions. Appl Clay Sci 1996; 11: 43-54.

[20] Sajidu SMI, Persson I, Masamba WRL, Henry EMT, Kayambazinthu D. Removal of Cd^{2+}, Cr^{3+}, Cu^{2+}, Hg^{2+}, Pb^{2+} and Zn^{2+} cations and AsO_4^{3-} anions from aqueous solutions by mixed clay from Tundulu in Malawi and characterization of the clay. Water Sanitation 2006; 32: 519-526.

[21] Srivastava P, Singh B, Angova M. Competitive adsorption behavior of heavy metals on kaolinite. J Colloid Interface Sci 2005; 290: 28-36.

[22] Zeng Z, Jiang J. Effects of the type and structure of modified clays on adsorption performance. Int J Environ Stud 2005; 62: 403-414.

[23] Pare S, Persson I, Guel B, Lundberg D, Zerbo L, Kam S, Traore K. Heavy metal removal from aqueous solutions by sorption using natural clays from Burkina Faso. African J Biotech 2012; 11: 10395-10406.

[24] Maguire M, Slaveck J, Vimpany I, Higginson FR, Pickering WF. Influence of pH on copper and zinc uptake by soil clays. Aust J Soil Res 1981; 19: 217-229.

[25] Coles CA, Yong RN. Aspects of kaolinite characterization and retention of Pb and Cd. Appl Clay Sci 2000; 22: 39-45.

[26] Echeverria JC, Zerranz I, Estella J, Garrido JJ. Simultaneous effect of pH, temperature, ionic strength, and initial concentration on the retention of lead on illite. Appl Clay Sci 2005; 30: 103-115.

[27] Hameed BH. Spent tea leaves: a new non-conventional and low-cost adsorbent for removal of basic dye from aqueous solutions. J Hazard Mater 2009; 161: 753-759.

[28] Onyango MS, Kojima Y, Aoyi O, Bernardo EC, Matsuda H. Adsorption equilibrium modeling and solution chemistry dependence of fluoride removal from water by trivalent cation-exchange zeolite F. J Colloid Interface Sci 2004; 279: 341-350.

[29] Treybal ER. Mass transfer operations. Singapore: McGraw-Hill; 1981.

[30] Pesquera C, Gonzalez F, Benito I, Blanco C, Mendioroz S, Pajares J. Passivation of a montmorillonite by the silica created in acid activation. J Mater Chem 1992; 2: 907-911.

[31] Lopez-Gonzalez JD, Deitz VR. Surface changes in an original and activated bentonite. J Res 1952; 48: 325-333.

[32] Leposava F, Perovic L. The effects of fine grinding on the physicochemical properties and thermal behavior of bentonite clay. J Serb Chem Soc 2002; 67: 753-760.

[33] Onal M. Changes in crystal structure, thermal behavior and surface area of bentonite by acid activation. Commun Fac Sci Univ Ank Series B 2007; 53: 1-14.

[34] Foletto EL, Volzone C, Porto LM. Performance of an Argentinian acid-activated bentonite in the bleaching of soybean oil. Braz J Chem Eng 2003; 20: 213-219.

[35] Giustetto R, Wahyudi O, Corazzari I, Turci F. Chemical stability and dehydration behavior of a sepiolite/indigo maya blue pigment. Appl Clay Sci 2011; 52: 41-48.

[36] Dikmen S, Yilmaz G, Yorukogullari E, Korkmaz E. Zeta potential study of natural- and acid-activated sepiolites in electrolyte solutions. Can J Chem Eng 2012; 90: 785-792.

[37] Anirudvan TS, Krishnan KA. Removal of cadmium II from aqueous solution by steam activated sulphurized carbon prepared from sugar-cane bagasse pith: kinetics and equilibrium studies. Water SA 2003; 29: 147-156.

[38] Nomanbhay SM, Palanisany K. Removal of heavy metal from industrial waste water using chitosan coated oil palm shell charcoal. Elect J Biotechnol 2005; 8: 43-53.

[39] Antunes WM, Luna SA, Henriques CA, Costa AC. An evaluation of copper biosorption by a brown seed weed under optimized conditions. Elect J Biotechnol 2003; 6: 174-184.

[40] Teker M, İmamoğlu M, Saltabaş Ö. Adsorption of copper and cadmium ions by activated carbon from rice husks. Turk J Chem 1999; 23: 185-191.

[41] Low KS, Lee CK, Kek KL. Removal of chromium VI from aqueous solution. Biores Technol 1995; 54: 133-139.

[42] Onwu FK, Ogah SPI. Studies on the effect of pH on the sorption of cadmium (II), nickel (II), lead (II), and chromium (VI) from aqueous solutions by African white star apple (*Chrysophyllum albidium*) shell. African J Biotech 2010; 9: 7086-7093.

[43] Ahmad A, Rafatullah M, Sulaiman O, Ibrahim MH, Hashim R. Scavenging behaviour of meranti sawdust in the removal of methylene blue from aqueous solution. J Hazard Mater 2009; 170: 357-365.

[44] Zohra B, Aicha K, Fatima S, Nourredine B, Zoubir D. Adsorption of Direct Red 2 on bentonite modified by cetyltrimethylammonium bromide. Chem Eng J 2008; 136: 295-305.

[45] Chaari I, Fakhfakh E, Chakroun S, Bouzid J, Boujelben N, Feki M, Rocha F, Jamoussi F. Lead removal from aqueous solution by Tunisian smectitic clay. J Hazard Mat 2008; 156: 545-551.

[46] Khenifi A, Bouberka Z, Kameche F, Derriche Z. Adsorption study of an industrial dye by an organic clay. Adsorption 2007; 13: 149-158.

[47] Ho YS, McKay G. The sorption of lead (II) ions on peat. Water Res 1999; 33: 578-584.

[48] Ozturk N, Kavak D. Adsorption of boron from aqueous solutions using fly ash: batch and column studies. J Hazard Mater 2005; B127: 81-88.

[49] Ho YS, McKay G. Sorption of dye from aqueous solution by peat. Chem Eng J 1998; 70: 115-124.

[50] Aharoni C, Sideman S, Hoffer E. Adsorption of phosphate ions by colloid coated alumina. J Chem Technol Biotechnol 1979; 29: 404-412.

[51] Karthikeyan T, Rajgopal S, Miranda LR. Chromium (VI) adsorption from aqueous solution by *Hevea Brasilinesis* sawdust activated carbon. J Hazard Mater B 2005; 124: 192-199.

[52] Ong SA, Seng CE, Lom V. Kinetic of adsorption of Cu(II) and Cd(II) from aqueous solution on rice husk and modified rice husk. Elect J Environ Agric Food Chem 2007; 6: 1764-1774.

[53] Arivoli S, Thenkuzhali M. Kinetic, mechanistics, thermodynamic and equilibrium studies on the adsorption of rhodamine B by acid activated low cost carbon. E-jour Chem 2008; 5: 187-200.

[54] Langmuir I. The constitution and fundamental properties of solids and liquids. J Am Chem Soc 1916; 38: 2221-2295.

[55] Aluyor EO, Oboh IO, Obahiagbon KO. Equilibrium sorption isotherm for lead (Pb) ions on hydrogen peroxide modified rice hulls. Int J Phys Sci 2009; 4: 423-427.

[56] Hall KR, Eagleton LC, Acrivos A, Vermeulen T. Pore and solid diffusion kinetics in fixed bed adsorption under constant pattern conditions. Ind Eng Chem Fundam 1966; 5: 212-223.

[57] Sumanjit K, Walia TPS, Mahanan RK. Comparative studies of zinc, cadmium, lead and copper on economically viable adsorbents. J Environ Eng Sci 2008; 7: 83-90.

[58] Malik PK. Dye removal from wastewater using activated carbon developed from sawdust: adsorption equilibrium and kinetics. J Hazard Mater 2004; 113: 81-88.

[59] Hema M, Arivoli S. Comparative study on the adsorption kinetics and thermodynamics of dyes onto acid activated low cost carbon. Int. J Phy Sci 2007; 2: 010-017.

[60] Mittal A, Mittal J, Kurup L. Utilization of hen feathers for the adsorption of Indigo Carmine from simulated effluents. J Environ Protect Sci 2007; 1: 92-100.

[61] Sivakumar P, Palanisamy PN. Adsorption studies of basic red 29 by a nonconventional activated carbon prepared from *Euphorbia antiquorum* L. Int J Chem Tech Res 2009; 1: 502-510.

[62] Babel S, Kurniawan TA. Cr(VI) removal from synthetic wastewater using coconut shell charcoal and commercial activated carbon modified with oxidizing agents and/or chitosan, Chemos 2004; 54: 951-967.

[63] Langmuir I. The adsorption of gases on plane surfaces of glass, mica and platinum. J Am Chem Soc 1918; 40: 1361-1403.

[64] Ho YS, Huang CT, Huang HW. Equilibrium sorption isotherm for metal ions on tree fern, Proc Biochem 2002; 37: 1421-1430.

[65] Juang LC, Wang CC, Lee CK, Hsu TC. Dyes adsorption onto organoclay and MCM-41. J Environ Engr Manage 2007; 17: 29-38.

[66] Khalid N, Ahmad S, Toheed A. Potential of rice husk for antimony removal. Appl Rad Isotope 2000; 52: 30-38.

[67] Temkin MJ, Pyzhev V. Kinetics of ammonia synthesis on promoted iron catalysis. Acta Physicochim USSR 1940; 12: 217-222.

[68] Basar CA. Applicability of the various adsorption models of three dyes adsorption onto activated carbon prepared from waste apricot. J Hazard Mater B 2006; 135: 232-241.

[69] Oladoja NA, Asia IO, Aboluwoye CO, Oladimeji B, Ashogbon AO. Studies on the sorption of basic dye by rubber (*Herea brasiliensis*) seed shell. Turkish J Eng Env Sci 2008; 32: 143-152.

[70] Lian L, Guo L, Guo C. Adsorption of congo red from aqueous solution on Ca-bentonite. J Hazard Mat 2009; 161: 126-131.